Millimeter- and submillimeter-wave spectroscopy of dibridged Si_2H_2 isotopomers: Experimental and theoretical structure

M. Bogey, H. Bolvin, M. Cordonnier, C. Demuynck, and J. L. Destombes
Université des Sciences et Technologies de Lille, Laboratoire de Spectroscopie Hertzienne, Associé au C.N.R.S., F-59655 Villeneuve d'Ascq Cedex, France

A. G. Császár
Department of Theoretical Chemistry, Eötvös Loránd University, H-1518 Budapest 112, P.O. Box 32, Hungary

(Received 31 January 1994; accepted 3 March 1994)

Various isotopomers of the free dibridged disilyne molecule, $Si(H_2)Si$, have been observed by millimeter- and submillimeter-wave spectroscopy in a silane–argon plasma produced by an abnormal electric discharge. In order to make measurement of the weak absorption lines possible a novel computer processing treatment has been developed. From the molecular constants measured for $^{28}Si(H_2)^{28}Si$, $^{29}Si(H_2)^{28}Si$, $^{30}Si(H_2)^{28}Si$, and $^{28}Si(D_2)^{28}Si$ an accurate substitution structure has been deduced with r_s(Si–Si)=2.2154 Å, r_s(Si–H)=1.6680 Å, and $\angle$(HSiSiH)=104.22°. The spectrum analysis and the structure determination have been aided by correlated level *ab initio* calculations resulting in accurate estimates of the equilibrium geometry and rotational constants, the cubic force field, the quartic and sextic centrifugal distortion constants, and the inversion barrier height of dibridged disilyne. The barrier to inversion of the "butterfly-type" $Si(H_2)Si$ molecule must be relatively high as no splitting due to inversion could be experimentally observed.

I. INTRODUCTION

High resolution spectroscopy is one of the conventional ways to obtain information about molecular energy levels and structures. Millimeter-wave (MMW) spectroscopy is inherently a very high resolution technique and makes possible the analysis of rotational and large amplitude vibrational motions of relatively small molecules in the gas phase. It leads to the determination of precise molecular parameters which can be employed to obtain an accurate estimate of equilibrium structures.

Due to the importance of species such as radicals, ions, and reactive molecules in the interstellar and circumstellar chemistry,[1,2] MMW and sub-MMW spectroscopy of reactive species has developed simultaneously with radio astronomy. The discovery of silicon compounds such as SiC_2, SiC, and SiC_4,[3–5] in the carbon-rich circumstellar envelope IRC +10216, indicated novel, intriguing features of silicon chemistry. Therefore, laboratory studies of silane and acetylene plasmas have been performed.[5–7] The importance of the processes leading to the formation of amorphous silicon films by chemical vapor deposition (CVD) or by plasma enhanced CVD in the microelectronics industry resulted in further interest in the special characteristics of silicon chemistry.

Certain differences between silicon and carbon chemistry lead to striking bridged structures of some unsaturated silicon compounds. These structures involve three center two electron bonds which are well known in molecules involving electron-deficient atoms, such as boron,[8] but quite little is known experimentally about such bonds in molecules containing group-IV elements. The only experimental result available is related to protonated acetylene, which has been investigated by infrared (IR)[9] and MMW spectroscopy,[10] and by Coulomb-explosion experiments.[11]

One of the simplest unsaturated silicon compounds is Si_2H_2, the formal all-silicon analog of acetylene. While the first spectroscopic evidence for disilyne was presented only in 1991,[12] theoretical investigations on the molecule have a much longer history. Early *ab initio* studies[13–16] suffered from the use of small basis sets and lack of electron correlation treatments. More recent *ab initio* studies[17–24] all revealed that sometimes even relatively small changes in the electron correlation treatments and basis sets have a substantial effect on the actual characteristic of the potential energy surface of Si_2H_2. Thus, it is not surprising that the theoretical studies of the seventies[13,14] erroneously predicted a linear, $D_{\infty h}$ symmetry configuration as the global minimum. Some years later, Snyder *et al.*[15] determined the geometries of five Si_2H_2 conformers on the lowest singlet surface. Their results, obtained at the Hartree–Fock (HF) and generalized valence-bond (GVB) levels of theory employing small basis sets, include: (a) the lowest energy form is disilavinylidene, H_2SiSi; (b) the linear form has the highest energy among the five conformers studied; and (c) these calculations were the first to indicate the existence of a bridged isomer, $Si(H_2)Si$. In the first detailed *ab initio* study, employing more extended basis sets and treatments for electron correlation of the low-lying structural isomers of the lowest singlet and triplet surfaces of Si_2H_2, Lischka and Köhler[17] provided firm evidence that the global minimum on the singlet surface belongs to the nonplanar dibridged isomer, $Si(H_2)Si$. This result was later confirmed in other theoretical studies.[18–24] Binkley[19] compared the relative stability of the various conformers of Si_2H_2 to that of C_2H_2 and concluded that the absence of a stable linear form for Si_2H_2 indicated that silicon is unwilling to participate in triple bonds. Clabo and Schaefer[20] mentioned Si_2H_2 in a work on hexasilabenzene and calculated the structural parameters for its various isomers. The most complete theoretical work on the isomers of Si_2H_2 is due to Colegrove and Schaefer,[21] who performed calculations at the self-

 0021-9606/94/100(12)/8614/11/$6.00

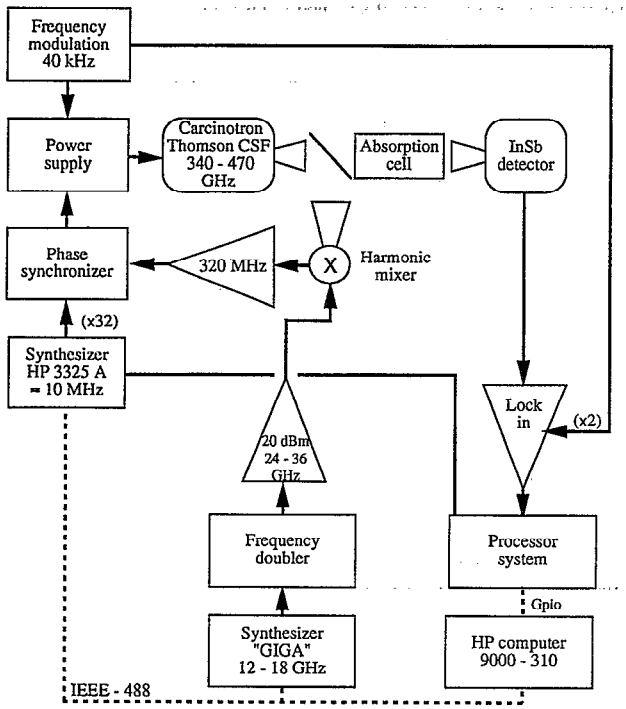

FIG. 1. Block diagram of the spectrometer.

consistent field (SCF) and configuration interaction singles and doubles (CISD) levels of theory using double-zeta plus polarization (DZP) and triple-zeta plus double polarization (TZ2P) basis sets. They found four stable structural isomers, the global minimum being the dibridged form which was experimentally observed in MMW spectroscopy by Bogey *et al.*.[12] Moreover, they discovered a new, astonishingly stable structure, whose relative energy, compared to $Si(H_2)Si$, was calculated to be rather small, only 10.8 kcal/mol. This so-called bridged-2 form has been experimentally observed in the Lille group[25] and was renamed to monobridged Si_2H_2.[22] Curtiss *et al.*[23] made a theoretical study on a number of Si_2H_n compounds and their results corroborated those of Colegrove and Schaefer[21] on $Si(H_2)Si$. Using state-of-the-art methodology, Handy and co-workers[24] calculated the ground state rotational constants and the infrared spectrum of $Si(H_2)Si$.

In this paper, we report a detailed spectroscopic and *ab initio* study of dibridged disilyne, $Si(H_2)Si$. The observation of MMW spectra of several isotopomers [$^{28}Si(H_2)^{28}Si$, $^{29}Si(H_2)^{28}Si$, $^{30}Si(H_2)^{28}Si$, and $^{28}Si(D_2)^{28}Si$] led to the determination of an accurate set of molecular parameters, from which a substitution r_s structure has been deduced. The spectrum analysis and the determination of molecular parameters have been aided by correlated level *ab initio* calculations, resulting in accurate estimates of the equilibrium geometry, rotational constants, cubic force field, quartic and sextic centrifugal distortion constants, and inversion barrier height of $Si(H_2)Si$. Finally, splitting of the rovibrational levels of $Si(H_2)Si$, due to an inversion-type large amplitude motion, is discussed based on group-theoretical arguments and *ab initio* data.

II. EXPERIMENT

A. Experimental setup

The MMW spectrum of very short-lived species can be detected only if these species are produced directly in the observation cell within a plasma excited by a dc glow discharge.

The observation cell consists of a 2.5 m long, 5 cm internal diameter Pyrex tube. Both ends are closed by two Teflon windows at the Brewster incidence to improve transmission and minimize standing waves. The temperature of the gas can be reduced to 77 K (without discharge) by flowing liquid nitrogen through a jacket surrounding the cell. Condensable gases are introduced through a small axial glass tube drilled all along its length.

The best conditions to observe the different isotopomers of $Si(H_2)Si$ were $P(SiH_4)=30$ mTorr (measured at room temperature) and $P(Ar)=20$ mTorr. The "abnormal" glow discharge[12] can be characterized by $V=3$ kV and $I=10$ mA.

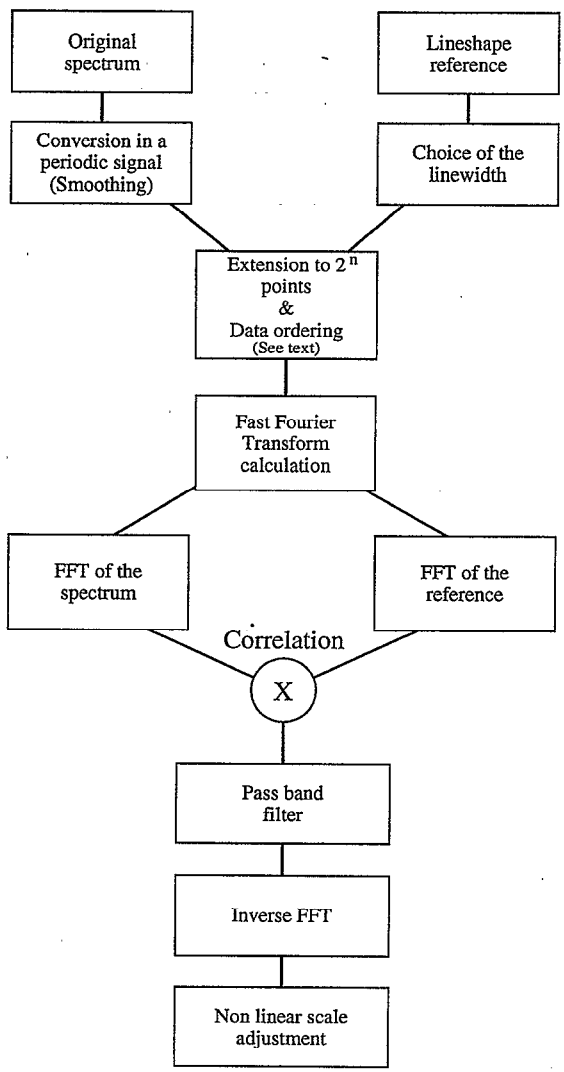

FIG. 2. Algorithm of the numerical treatment.

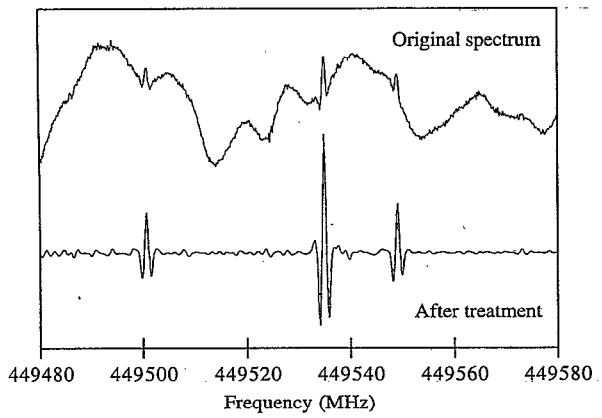

FIG. 3. A spectrum before and after data processing with (1) the dibridged $Si(H_2)Si$ line: $3_{2,2}\leftarrow3_{1,2}$ at 449 500.642 MHz, (2) the monobridged Si(H)SiH lines: $31_{2,30}\leftarrow30_{2,29}$ at 449 534.834 MHz, and (3) $31_{4,28}\leftarrow30_{4,27}$ and $30_{4,27}\leftarrow30_{4,26}$ at 449 549.032 MHz.

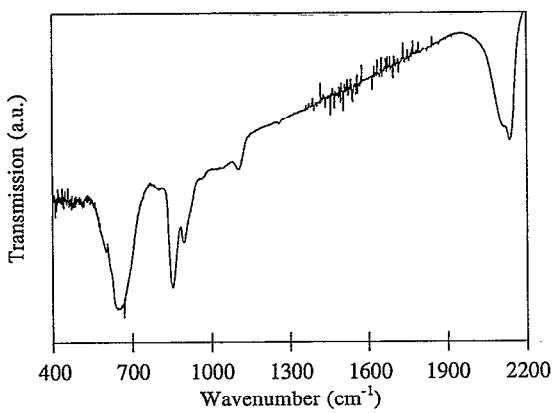

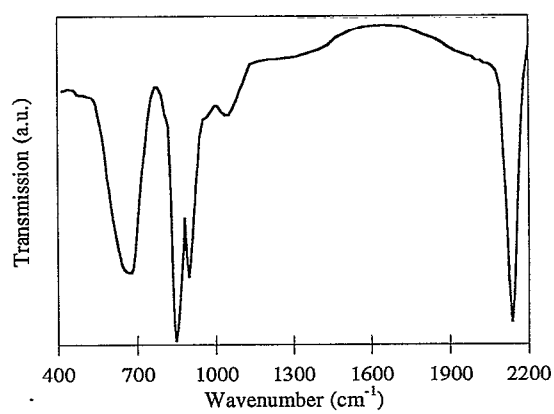

FIG. 4. (a) IR spectrum of a film deposited in our cell. Experimental conditions: $T\approx120$ K, $P(SiH_4)=30$ mTorr, $P(Ar)=20$ mTorr, $V\approx3$ kV, $I\approx10$ mA. Note that the noise of this spectrum is mainly due to an imperfect subtraction of the water absorption (b) IR spectrum of an *a*-Si:H deposit taken from Ref. 27.

TABLE I. Representations of symmetric powers of Γ_{vib} for dibridged Si_2H_2.

C_{2v}	E	C_2	$\sigma_v(xz)$	$\sigma_v(yz)$	Species
Γ_{vib}	6	2	2	2	$3A_1+A_2+B_1+B_2$
$[\Gamma^2_{vib}]$	21	5	5	5	$9A_1+4A_2+4B_1+4B_2$
$[\Gamma^3_{vib}]$	56	8	8	8	$20A_1+12A_2+12B_1+12B_2$

TABLE II. Symmetry coordinates for dibridged Si_2H_2.[a]

Sym.	No.	Internal coordinate	Description
a_1	1	$r_{13}+r_{14}+r_{23}+r_{24}$	SiH str
	2	$\alpha_{132}-\alpha_{324}+\alpha_{241}-\alpha_{413}$	Ring bend
	3	$\tau_{1324}-\tau_{3241}+\tau_{2413}-\tau_{4132}$	Ring bend
a_2	4	$r_{13}-r_{14}-r_{23}+r_{24}$	SiH str
b_1	5	$r_{13}-r_{14}+r_{23}-r_{24}$	SiH str
b_2	6	$r_{13}+r_{14}-r_{23}-r_{24}$	SiH str

[a]The atomic numbering is $Si_1(H_3,H_4)Si_2$. Normalization factors have been omitted. The torsional coordinate, τ_{ijkl}, is positive when, viewed in the direction $k\rightarrow j$, $\mathbf{r}_{kl}$ rotates counterclockwise with respect to $\mathbf{r}_{ji}$.

TABLE III. Geometries and dipole moments for dibridged Si_2H_2.

	r(Si–Si) (Å)	r(Si–H) (Å)	∠(HSiSiH) (deg)	μ (D)	Reference
Experiment					
r_0 structure	2.2079	1.6839	103.18		12
r_s structure	2.2154	1.6680	104.22		This work
Theory					
DZP SCF	2.185	1.674	102.1	0.403	This work
TZ2P SCF	2.189	1.679	102.8	0.478	This work
TZ2P CISD	2.214	1.667	103.6	0.427	This work
TZ2P CISD	2.216	1.668	104.0		21[a]
TZ2P+f CCSD(T)	2.222	1.681	106.5	0.343	22
TZ2P+f BD	2.1966	1.6654	104.15		24[b]

[a]The small differences between the present TZ2P CISD results and those of Colegrove and Schaefer (Ref. 21) are due to the different selection of active orbitals for the correlated calculation.

[b]Hühn *et al.* (Ref. 24) used the Brueckner (BD) variant of coupled cluster theory and a TZ2P+f basis whose TZ2P part is different from the TZ2P basis set used in this study.

TABLE IV. Theoretical cubic force fields of dibridged Si_2H_2 in symmetry coordinates.[a]

Constant	DZP SCF	TZ2P CISD	Constant	DZP SCF	TZ2P CISD
11	2.078	1.948	223	−2.197	−1.826
12	1.023	0.897	133	−1.494	−1.257
22	1.552	1.337	233	−1.989	−1.550
13	0.658	0.549	333	−2.632	−2.000
23	0.527	0.399	144	−2.759	−2.720
33	0.686	0.503	244	0.049	0.089
44	0.697	0.824	344	0.424	0.403
55	1.302	1.245	155	−3.108	−3.046
66	0.946	0.959	255	−0.799	−0.694
111	−4.565	−4.387	355	−0.354	−0.302
112	−1.829	−1.654	456	−2.851	−2.900
122	−2.265	−2.049	166	−2.656	−2.588
222	−3.110	−2.668	266	0.192	0.287
113	−1.227	−1.071	366	0.181	0.197
123	−1.352	−1.155			

[a]Internal coordinate force constants ($ijk,\{i,j,k\in[1,6]\}$) correspond to energy measured in aJ, distances in Å and angles in rad. For the definition of the symmetry coordinates see Table II.

TABLE V. *Ab initio* molecular constants of $^{28}Si_2H_2$ and $^{28}Si_2D_2$ dibridged and comparison with experiment.

	$^{28}Si_2H_2$				$^{28}Si_2D_2$	
	This work TZ2P CISD	Hühn *et al.*[a] TZ2P+f BD	Grev and Schaefer[b] TZ2P+f CCSD(T)	Experiment (this work)	This work TZ2P CISD	Experiment (this work)
A (MHz)	163 535.76	163 588	159 602	157 198.8668	82 874.73	80 575.1920
B (MHz)	7249.37	7364	7192	7281.326 47	7139.14	7180.278 25
C (MHz)	7169.28	7275	7112	7199.733 96	6978.09	7014.327 80
Δ_J (kHz)	5.1352	4.8782	5.420	5.697 68	4.6872	5.1716
Δ_{JK} (kHz)	−52.041	−32.432	−65.13	−61.704	3.804	−1.897
Δ_K (kHz)	9220.46	8134.8	8980	8844.6	2306.60	2251.58
δ_J (kHz)	0.002 589	0.014 34	−0.002 132	−0.004 247	0.012 98	0.004 29
δ_K (kHz)	47.77	43.36	52.32	62.57	42.21	52.40
Φ_J (Hz)	0.0006	···	···		0.0005	
Φ_{JK} (Hz)	0.3858	···	···	0.607	0.197	0.281
Φ_{KJ} (Hz)	−54.31	···	···	−62.1	−16.13	−17.7
Φ_K (Hz)	1365.6	···	···	1040	178.83	226
ϕ_J (Hz)	0.0000	···	···		0.0001	
ϕ_{JK} (Hz)	0.1831	···	···		0.1410	
ϕ_K (Hz)	15.98	···	···		6.452	

[a]Reference 24.
[b]Reference 22.

$Si(D_2)Si$ was produced employing the same experimental conditions as above and replacing SiH_4 by SiD_4.

Detection of reactive species which are always produced in low concentration requires a spectrometer with very high sensitivity. The Lille group has recently completed development of a new version of a computer-controlled spectrometer described below.

Below 340 GHz, harmonic generation from klystrons or Gunn oscillators emitting in the 50–75 GHz frequency range is used. The sources are phase locked on the emission of a 12–18 GHz synthesizer (Giga Instrument) by comparing the IF frequency beat near 320 MHz with the emission of a 3325B Hewlett–Packard synthesizer. Small frequency scans are obtained by sweeping the emission of the HP synthesizer. For large frequency scans the same technique is used together with step incrementation of the Giga synthesizer.

Above 340 GHz, two carcinotrons from Thomson CSF emitting in the 340–470 GHz frequency range are used. They are phase locked on the second harmonic of the Giga synthesizer (see Fig. 1). The high power delivered by these carcinotrons allows achievement of very high sensitivity (typically 10^{-8} cm^{-1} for a 10 Hz bandwidth detection).

Detection is achieved by a helium cooled InSb detector from QMC Instruments. The emission of all the millimeter and submillimeter sources are frequency modulated at 40 kHz, while the signal is demodulated at twice this frequency providing a second derivative line shape.

A HP 9000-310 microcomputer is interfaced through a microprocessor to a A/D converter, and also drives the synthesizers. It automatically sweeps the frequency of the MMW source and simultaneously records the spectrum. It is then possible to use computer processing to improve the S/N ratio and to measure the frequency of the lines.

B. Computer-controlled data processing

In this type of experiment, the major limitation to sensitivity is due to the presence of standing waves which have an amplitude much larger than the weak absorption signal searched for. The Lille group developed a computer-

TABLE VI. Theoretical barrier heights to inversion of dibridged Si_2H_2.[a]

Basis	E_{SCF}	ΔMP2	ΔMP3	ΔMP4	ΔMP∞	$E_{MP\infty}$	ΔCCSD	ΔCCSD(T)	$E_{CCSD(T)}$	ΔCISD	ΔCISD+Q	E_{CISD+Q}
6-31G* (42)	7457	−2582	111	−396	−79	4511	−2414	−344	4699	−1830	−719	4908
DZP (58)	6811	−2566	174	−410	−76	3934	−2352	−378	4081			
TZ2P (84)	6200	−2512	213	−347	−53	3502	−2110	−463	3627	−1611	−603	3900
TZ2P+R (94)	6194	−2489	221	−348	−53	3525	−2083	−459	3652			
cc-pVTZ (96)	6035	−2193	317	−327	−41	3792	−1644	−461	3930			
TZ2P+R+fd (126)	6162	−2173	336	−365	−50	3909	−1650	−458	4054			
cc-pVQZ (178)	5891						−1477	−467	3947			

[a]All energy values in cm^{-1}. All single point energy calculations were performed at the TZ2P CISD optimized theoretical structures. The ΔMP2, ΔMPn, ΔCCSD, ΔCCSD(T), ΔCISD, and ΔCISD+Q values refer to energy differences $E_{MP2}-E_{SCF}$, $E_{MPn}-E_{MPn-1}$, $E_{CCSD}-E_{SCF}$, $E_{CCSD(T)}-E_{CCSD}$, $E_{CISD}-E_{SCF}$, and $E_{CISD+Q}-E_{CISD}$, respectively. The E_{SCF}, $E_{MP\infty}$, $E_{CCSD(T)}$, and E_{CISD+Q} values represent barrier heights obtained at the respective levels of theory.

TABLE VII. Rotational frequencies of dibridged $^{28}Si(H_2)^{28}Si$ (in MHz) with the differences $\Delta f = f_m - f_c$ (in MHz). The standard deviation of the fit is $\sigma = 21$ kHz.

J	K_a	K_c	J	K_a	K_c	f_m	Δf
14	1	14	14	0	14	145 737.463(50)	0.013
13	1	13	13	0	13	146 293.790(50)	−0.004
12	1	12	12	0	12	146 811.878(50)	0.029
11	1	11	11	0	11	147 291.294(50)	0.000
10	1	10	10	0	10	147 731.832(50)	0.003
9	1	9	9	0	9	148 133.198(50)	0.015
8	1	8	8	0	8	148 495.142(50)	0.034
7	1	7	7	0	7	148 817.377(50)	−0.003
5	1	5	5	0	5	149 342.165(50)	−0.033
3	1	3	3	0	3	149 706.289(50)	−0.061
4	1	3	3	0	3	208 280.277(50)	−0.025
6	1	5	5	0	5	237 688.293(50)	0.003
7	1	6	6	0	6	252 452.763(50)	0.012
8	1	7	7	0	7	267 257.511(50)	−0.009
11	2	9	12	1	11	272 887.505(50)	0.007
10	1	9	9	0	9	296 988.123(50)	−0.004
9	2	7	10	1	9	302 746.230(50)	0.027
11	1	10	10	0	10	311 914.107(50)	0.009
8	2	7	9	1	9	321 273.440(50)	−0.054
12	1	11	11	0	11	326 880.643(50)	−0.002
13	1	12	12	0	12	341 887.898(50)	0.004
27	3	25	28	2	27	344 708.635(50)	−0.009
6	2	4	7	1	6	347 253.911(50)	0.062
6	2	5	7	1	7	349 529.142(50)	−0.012
14	1	13	13	0	13	356 936.007(50)	0.007
26	3	23	27	2	25	358 312.601(50)	0.008
5	2	3	6	1	5	362 013.187(50)	−0.008
5	2	4	6	1	6	363 720.265(50)	0.020
16	1	15	15	0	15	387 155.536(50)	0.022
24	3	21	25	2	23	387 298.457(50)	0.013
3	2	1	4	1	3	391 414.862(50)	−0.016
17	1	16	16	0	16	402 327.364(50)	0.014
22	3	19	23	2	21	416 270.064(50)	−0.030
22	3	20	23	2	22	416 684.509(50)	−0.013
18	1	17	17	0	17	417 540.876(50)	−0.021
38	2	37	38	1	37	420 154.508(50)	0.003
36	2	35	36	1	35	423 122.673(50)	−0.024
34	2	33	34	1	33	425 938.391(50)	0.010
32	2	31	32	1	31	428 600.519(50)	0.007
21	3	18	22	2	20	430 751.698(50)	0.040
21	3	19	22	2	21	431 099.941(50)	0.013
30	2	29	30	1	29	431 108.150(50)	0.021
19	1	18	18	0	18	432 796.408(50)	−0.020
28	2	27	28	1	27	433 460.389(50)	0.036
27	2	26	27	1	26	434 577.910(50)	−0.028
26	2	25	26	1	25	435 656.364(50)	−0.016
25	2	24	25	1	24	436 695.600(50)	0.012
24	2	23	24	1	23	437 695.474(50)	−0.004
23	2	22	23	1	22	438 655.978(50)	0.008
22	2	21	22	1	21	439 577.000(50)	0.014
21	2	20	21	1	20	440 458.400(50)	−0.053
20	2	19	20	1	19	441 300.283(50)	−0.021
19	2	18	19	1	18	442 102.446(50)	−0.026
18	2	17	18	1	17	442 864.901(50)	0.004
17	2	16	17	1	16	443 587.538(50)	0.018
16	2	15	16	1	15	444 270.301(50)	0.014
15	2	14	15	1	14	444 913.140(50)	−0.007
20	3	17	21	2	19	445 230.895(50)	−0.013
14	2	13	14	1	13	445 516.052(50)	−0.001
20	3	18	21	2	20	445 521.273(50)	0.023
13	2	12	13	1	12	446 078.958(50)	−0.003
12	2	11	12	1	11	446 601.820(50)	−0.008
11	2	10	11	1	10	447 084.610(50)	−0.008
10	2	9	10	1	9	447 527.295(50)	−0.001
9	2	8	9	1	8	447 929.818(50)	−0.011
20	1	19	19	0	19	448 094.257(50)	0.015
8	2	7	8	1	7	448 292.191(50)	0.001
7	2	6	7	1	6	448 614.337(50)	−0.016
6	2	5	6	1	5	448 896.295(50)	0.000
5	2	4	5	1	4	449 138.021(50)	0.025
4	2	3	4	1	3	449 339.436(50)	−0.003
3	2	2	3	1	2	449 500.642(50)	0.032
2	2	1	2	1	1	449 621.499(50)	0.000
2	2	0	2	1	2	449 865.560(50)	0.001
3	2	1	3	1	3	449 988.827(50)	−0.003
4	2	2	4	1	4	450 153.326(50)	−0.032
5	2	3	5	1	5	450 359.283(50)	−0.005
6	2	4	6	1	6	450 606.802(50)	0.003
7	2	5	7	1	7	450 896.100(50)	−0.006
8	2	6	8	1	8	451 227.459(50)	0.000
9	2	7	9	1	9	451 601.146(50)	−0.001
10	2	8	10	1	10	452 017.499(50)	0.008
11	2	9	11	1	11	452 476.856(50)	0.007
12	2	10	12	1	12	452 979.619(50)	0.003
13	2	11	13	1	13	453 526.225(50)	0.005
14	2	12	14	1	14	454 117.131(50)	0.004
15	2	13	15	1	15	454 752.841(50)	0.004
16	2	14	16	1	16	455 433.883(50)	−0.002
17	2	15	17	1	17	456 160.847(50)	0.005
18	2	16	18	1	18	456 934.343(50)	0.030
19	2	17	19	1	19	457 754.943(50)	0.004
20	2	18	20	1	20	458 623.382(50)	−0.012
21	2	19	21	1	21	459 540.395(50)	0.006
19	3	16	20	2	18	459 708.176(50)	−0.036
19	3	17	20	2	19	459 948.155(50)	0.005
22	2	20	22	1	22	460 506.669(50)	0.002
23	2	21	23	1	23	461 523.018(50)	0.011
24	2	22	24	1	24	462 590.202(50)	−0.016
21	1	20	20	0	20	463 434.660(50)	0.000
25	2	23	25	1	25	463 709.142(50)	−0.004
26	2	24	26	1	26	464 880.612(50)	−0.057
27	2	25	27	1	27	466 105.713(50)	0.016
28	2	26	28	1	28	467 385.191(50)	0.018
29	2	27	29	1	29	468 720.086(50)	0.015
30	2	28	30	1	30	470 111.402(50)	0.005
31	2	29	31	1	31	471 560.178(50)	−0.009

controlled data processing to circumvent this problem. The procedure is based on a cross-correlation routine between a spectrum sample and a reference line shape. The basic idea of this treatment is to extract any sample that "looks like" a reference line shape, or in other words that is correlated with it, from the experimental spectrum.

Because second harmonic demodulation technique is employed, the reference line should have a second derivative Voigt profile. In the present case, a second derivative Gaussian line shape is a good approximation of the observed line shape and is faster to calculate. Its width is preliminarily chosen by comparison with other intense line(s) observed in the same frequency range.

The most efficient way to calculate this correlation is to use a procedure based on a fast Fourier transform (FFT) routine. However, this involves the approximation that the signals observed are periodic. Since, this is not true for the experimental spectrum, one first needs to smooth its start and

its end to the same value in order to remove any discontinuity that would affect the FFT treatment.

The FFT calculations are made using a conventional routine[26] that allows simultaneous calculation of the FFT of the spectrum and of the reference line shape. This FFT calculation supposes to extend the data up to 2^n points (where n is an integer), and to proceed to some special ordering of these data. Just before doing the inverse FFT that gives the final result, some additional low- and high-pass filters are used to remove the residual noise (see Fig. 2).

The treatment described does not preserve the original line shapes. Nevertheless, the principal advantage of second derivative line profiles is that their visual appearance is maintained after correlation and thus facilitates the interpretation of a treated spectrum.

Lines are extracted, as well as any sample of the record that accidentally looks like a line. In the case of the search for very weak lines, one can overcome this problem by comparing two successive scans of the same frequency range after and, of course, before treatment. Furthermore, to improve the contrast between extracted lines and the residual noise, one can use an adjustable nonlinear scale for the intensity. Figure 3 shows a typical scan before and after data processing.

C. Film deposition by silane plasma

In order to ascertain whether the characteristics of the glow discharge employed in this study differ from those used in the studies of *a*-Si:H alloys, the infrared spectrum of a film deposited on a crystalline silicon wafer placed into the cell during the spectroscopic experiments has been measured. The spectrum obtained is rather similar to that obtained by Lucovsky *et al.*[27] at approximately the same temperature (−125 °C) (Fig. 4). It suggests that $Si(H_2)Si$ could be one of the species involved in the chemical processes of silane plasmas commonly used for CVD deposition, as already indicated by mass spectrometric studies of Robertson and Gallagher.[28]

III. COMPUTATIONAL DETAILS

Several basis sets have been used in this study. The smallest basis, designated, as usual, 6-31G* (42 contracted Gaussian functions, CGFs), is that of Pople *et al.*[29] The DZP basis (58 CGFs) contains the usual DZ basis of Huzinaga[30] and Dunning,[31,32] augmented with one set of p and Cartesian d functions with orbital exponents $\alpha_p(H)=0.75$ and $\alpha_d(Si)=0.50$. The TZ2P basis (84 CGFs) contains the McLean and Chandler's $6s5p$ contraction[33] of Huzinaga's $12s9p$ primitive set for Si, augmented with two sets of Cartesian d functions with orbital exponents $\alpha_d(Si)=1.0$ and 0.25, and the $3s$ contraction of Huzinaga's $5s$ primitive set for H, augmented with two sets of p functions with exponents $\alpha_p(H)=1.50$ and 0.375. The TZ2P+R (94 CGFs) basis consists of the TZ2P basis above plus diffuse functions on Si and H [$\alpha_s(Si)=0.0347$, $\alpha_p(Si)=0.0230$, and $\alpha_s(H)=0.0483$].[20] The TZ2P+R+fd basis (126 CGFs) contains, in addition to the TZ2P+R set, a set of Cartesian f functions on Si [$\alpha_f(Si)=0.320$] and a set of Cartesian d functions on H [$\alpha_d(H)=1.0$].[20] The cc-pVTZ (96 CGFs) and cc-pVQZ (178 CGFs) basis sets are the correlation-consistent polarized valence triple-zeta and quadruple-zeta sets, respectively, of Dunning and co-workers,[34,35] containing pure d, f, and g functions.

While the calculated harmonic frequencies of Si_2H_2 bear indications of a multireference problem,[24] the t_1 diagnostic values of coupled cluster theory[36] are around 0.018 for $Si(H_2)Si$, suggesting that dibridged disilyne can adequately be described by single-reference-based electron-correlation treatments. Therefore, reference electronic wave function were determined in this study by the single-reference, self-consistent-field (SCF), restricted Hartree–Fock (HF) method.[37,38] Dynamic electron correlation was accounted for by Møller–Plesset perturbation theory through fourth order [MP2, MP3, and MP4(SDTQ)],[38–41] by the configuration interaction singles and doubles (CISD) methods,[38,42,43] and by the coupled-cluster singles and doubles method (CCSD)[41,44,45] augmented, in some cases, with the addition of a perturbative contribution from connected triple excitations [CCSD(T)].[46,47] In some cases, designated CISD+Q, the Davidson correction[48] was appended to the CISD energy to estimate the unlinked cluster contribution from quadruple excitations. In the cases labeled MP∞, the exact correlation energy (E_{corr}) within a given one-particle basis set was estimated by extrapolating the MP series according to the formula $E_{corr}=(E_2+E_3)/(1-E_4/E_2)$[49,50] where E_n represents the nth-order correction to the electronic energy.

Not all the electrons have been correlated explicitely in the MP, CI, and CC calculations: The ten lowest-energy core-like orbitals (corresponding to $1s$, $2s$, and $2p$ for Si, and $1s$ for H) and the two highest-energy virtual orbitals (corresponding to $1s^*$ of H) were always excluded.

The program packages PSI[51] and ACES II[52] have been utilized for the electronic structure calculations.

Group theory[53–55] has been used to determine the number of geometry parameters (3), and independent quadratic (9) and cubic (20) force constants (see Table I). The symmetry coordinates of dibridged Si_2H_2 are listed in Table II. The geometries were optimized by analytic gradient methods (SCF and CISD) until the largest internal coordinate force was smaller than 10^{-7} mdyn (Table III). The DZP SCF and TZ2P CISD cubic force fields were derived from analytic first derivative calculations using appropriate finite difference formulas (Table IV). To avoid complications resulting from the nonzero force dilemma[56] the force fields were evaluated at the respective optimized geometries. Transformation of the anharmonic force fields between the different coordinate systems was performed using the program INTDER.[56,57] Calculation of the spectroscopic constants was performed using well-known formulas obtained from second-order perturbation theory[58–61] (Table V). The results concerning the inversion barrier height are given in Table VI.

TABLE VIII. Rotational frequencies of dibridged $^{29}Si(H_2)^{28}Si$ and $^{30}Si(H_2)^{28}Si$ (in MHz) with the differences $\Delta f = f_m - f_c$ (in MHz). The standard deviations of the fits are σ=54 and 61 kHz, respectively.

						$^{29}Si(H_2)^{28}Si$		$^{30}Si(H_2)^{28}Si$	
J	K_a	K_c	J	K_a	K_c	f_m	Δf	f_m	Δf
14	1	13	13	0	13	353 457.095(200)	0.029	350 213.596(200)	0.083
18	1	17	17	0	17	412 991.971(200)	−0.049	408 751.741(200)	−0.081
20	1	19	19	0	19	443 001.097(200)	0.015	438 254.011(200)	−0.061
18	2	17	18	1	17	443 354.425(200)	0.043	443 807.245(200)	0.036
16	2	15	16	1	15	444 711.116(200)	−0.027	445 119.398(200)	−0.014
14	2	13	14	1	13	445 913.727(200)	−0.041	446 282.487(200)	−0.024
12	2	11	12	1	11	446 961.898(200)	−0.019	447 296.156(200)	−0.030
10	2	9	10	1	9	447 855.299(200)	0.005	448 160.173(200)	0.008
8	2	7	8	1	7	448 593.688(200)	0.034		
6	2	5	6	1	5	449 176.816(200)	0.023		
5	2	3	5	1	5	450 589.328(200)	−0.021		
7	2	5	7	1	7	451 107.686(200)	−0.079		
9	2	7	9	1	9	451 788.560(200)	0.024	451 964.575(200)	0.035
11	2	9	11	1	11	452 633.935(200)	0.001	452 782.163(200)	−0.004
13	2	11	13	1	13	453 646.792(200)	0.030	453 761.511(200)	−0.011
15	2	13	15	1	15	454 830.483(200)	0.129		
17	2	15	17	1	17	456 188.501(200)	−0.072		
19	2	17	19	1	19	457 725.775(200)	−0.029		
22	1	21	21	0	21	473 174.119(200)	0.008	467 914.466(200)	0.069

IV. RESULTS

A. Analysis of the spectra and molecular structure

Extending the first detection of dibridged disilyne by the Lille group,[12] a total of 106 *c*-type rotational transitions of $Si(H_2)Si$, characterized by $J \leqslant 38$ and $K_a \leqslant 3$, have been observed in this study (see Table VII).

Owing to the C_{2v} symmetry of $Si(H_2)Si$, its structure is completely determined by three parameters (cf. Tables I and III) and a r_0 structure could be deduced from the experimental rotational constants A_0, B_0, and C_0. In order to confirm the molecular identification, this structure has been used to predict the spectra of the other isotopomers $^{28}Si(H_2)^{29}Si$, $^{28}Si(H_2)^{30}Si$, and $^{28}Si(D_2)^{28}Si$.

The spectra of the ^{29}Si and ^{30}Si substituted species were observed in natural abundance (4.70% and 3.09%, respectively), and the frequencies of 19 and 12 transitions were measured (see Table VIII). For $Si(D_2)Si$, a total number of 60 lines characterized by $J \leqslant 24$ and $K_a \leqslant 5$, have been measured (see Table IX).

The lines of these various isotopomers have been fitted to Watson's *A*-reduced Hamiltonian.[62] The molecular constants obtained are presented in Table X. They are in good agreement with theoretical values both for $Si(H_2)Si$ and $Si(D_2)Si$ (see Table V). They also compare favorably with the *ab initio* values of Grev and Schaefer[22] and of Hühn *et al.*[24] in the case of $Si(H_2)Si$ (Table V). The few larger-than-usual differences between theory and experiment observed for certain centrifugal distortion constants are worth discussing. One of them concerns the very small δ_J constant: while the TZ2P CISD and TZ2P+f BD[24] values for $Si(H_2)Si$ do not have the correct sign, Grev and Schaefer[22] obtained the good sign at their ANO CCSD(T) level, but their absolute value is two times smaller than the experimental one. Furthermore, for $Si(D_2)Si$ the TZ2P CISD value of δ_J differs from experiment by a factor of 3 and now Δ_{JK} does not have the correct sign. These problems should probably be traced back to the occasional sensitivity of the calculated centrifugal distortion constants to small differences in the force fields and in the underlying geometries determined at different levels of theory.[63] Concerning the three sextic centrifugal distortion constants which could be determined experimentally, the agreement between experiment and theory is satisfactory for both species.

Observation of the isotopically substituted forms confirms undoubtedly the identification of $Si(H_2)Si$ and its dibridged structure (Fig. 5). The rotational constants determined for the four species (Table X) were employed to determine a r_s substitution structure for $Si(H_2)Si$. The structural parameters obtained are compared in Table III with the r_0 and *ab initio* results. The overall agreement between experiment and theory is remarkably good. Note that the extremely small differences between the r_s and TZ2P CISD structures are due to a fortuitous error cancellation at this level of theory.

B. Barrier to inversion

The butterfly structure of $Si(H_2)Si$ makes possible an inversion-type large amplitude motion. The complete nuclear permutation-inversion (CNPI) group of $Si(H_2)Si$, which contains all permutations and permutation inversions of the two identical nuclei H and Si, is composed of eight operations: E, (12), (ab), $(12)(ab)$, E^*, $(12)^*$, $(ab)^*$, and $(12)(ab)^*$ where operations (12) and (ab) represent the permutation of the two equivalent protons and silicons, respectively, and E^* is the inversion operation. This group, denoted as $\mathscr{D}_{2h}(M)$, is isomorphic with the $\mathscr{D}_{2h}$ point group, which corresponds to the planar reference configuration of $Si(H_2)Si$ at the midpoint of the hypothetical tunneling motion. It contains the

TABLE IX. Rotational frequencies of dibridged $^{28}Si(D_2)^{28}Si$ (in MHz) with the differences $\Delta f = f_m - f_c$ (in MHz). The standard deviation of the fit is $\sigma = 19$ kHz.

J	K_a	K_c	J	K_a	K_c	f_m	Δf
11	4	7	12	3	9	343 629.616(200)	0.004
11	4	8	12	3	10	343 631.136(200)	0.056
18	1	17	17	0	17	343 771.124(50)	0.005
9	2	7	8	1	7	345 246.737(50)	0.008
9	2	8	8	1	8	351 120.929(50)	−0.013
10	4	6	11	3	8	357 822.116(100)	−0.049
10	2	8	9	1	8	358 737.294(50)	−0.003
19	1	18	18	0	18	359 706.556(50)	−0.001
28	3	26	28	2	26	361 876.951(50)	0.000
24	3	22	24	2	22	364 289.985(50)	0.000
20	3	18	20	2	18	365 791.980(50)	0.002
16	3	14	16	2	14	366 635.438(50)	−0.003
10	3	8	10	2	8	367 145.043(50)	0.001
9	3	7	9	2	7	367 177.779(50)	−0.004
8	3	6	8	2	6	367 201.581(50)	0.004
7	3	5	7	2	5	367 218.207(50)	−0.011
6	3	4	6	2	4	367 229.304(50)	0.005
5	3	3	5	2	3	367 236.212(50)	−0.002
4	3	2	4	2	2	367 240.175(50)	0.020
3	3	1	3	2	1	367 242.132(200)	0.015
3	3	0	3	2	2	367 243.515(100)	−0.001
4	3	1	4	2	3	367 244.366(100)	0.013
5	3	2	5	2	4	367 246.010(50)	−0.001
6	3	3	6	2	5	367 248.895(80)	−0.007
7	3	4	7	2	6	367 253.518(50)	−0.002
8	3	5	8	2	7	367 260.438(50)	−0.004
9	3	6	9	2	8	367 270.323(50)	−0.010
10	3	7	10	2	9	367 283.936(50)	−0.007
15	3	12	15	2	14	367 440.322(50)	0.003
19	3	16	19	2	18	367 742.620(50)	0.023
23	3	20	23	2	22	368 308.857(50)	−0.010
3	3	0	2	2	0	409 826.657(200)	0.117
3	3	1	2	2	1	409 826.657(200)	−0.163
13	2	12	12	1	12	411 358.289(50)	−0.009
16	5	11	17	4	13	419 229.321(100)	0.021
16	5	12	17	4	14	419 229.321(100)	−0.031
4	3	1	3	2	1	424 019.895(100)	−0.005
4	3	2	3	2	2	424 021.287(100)	−0.010
23	1	22	22	0	22	424 615.278(100)	−0.016
15	2	13	14	1	13	425 236.675(50)	−0.007
14	2	13	13	1	13	426 623.442(50)	−0.027
15	5	10	16	4	12	433 414.229(50)	0.007
15	5	11	16	4	13	433 414.229(50)	−0.025
5	3	2	4	2	2	438 211.728(50)	0.003
5	3	3	4	2	3	438 215.923(50)	0.011
16	2	14	15	1	14	438 372.043(50)	−0.005
24	1	23	23	0	23	441 151.141(50)	0.000
15	2	14	14	1	14	441 971.163(50)	0.040
14	5	10	15	4	12	447 600.028(50)	0.013
14	5	9	15	4	11	447 600.028(50)	0.032
17	2	15	16	1	15	451 462.666(50)	0.013
6	3	3	5	2	3	452 401.172(50)	0.036
6	3	4	5	2	4	452 410.923(50)	0.022
16	2	15	15	1	15	457 401.350(50)	−0.006
25	1	24	24	0	24	457 817.379(50)	0.001
13	5	8	14	4	10	461 786.618(50)	−0.005
13	5	9	14	4	11	461 786.618(50)	−0.017
18	2	16	17	1	16	464 513.367(50)	−0.005
7	3	4	6	2	4	466 587.043(50)	−0.016
7	3	5	6	2	5	466 606.524(60)	−0.052

subgroup $\mathscr{C}_{2v}$ which corresponds to the two symmetrically equivalent equilibrium structures of the molecule (see Fig. 6). The molecular symmetry group $\mathscr{C}_{2v}(M)$, isomorphic with the $\mathscr{C}_{2v}$ point group, of one of these two equivalent (A) and (B) forms is $\{E, (12)(ab), (12)^*, (ab)^*\}$. It contains only the elements of the CNPI group that do not interconvert the two (A) and (B) forms. The reverse correlation table from $\mathscr{C}_{2v}(M)$ to $\mathscr{D}_{2h}(M)$

$\mathscr{C}_{2v}(M)$	$\mathscr{D}_{2h}(M)$
A_1	$A_g \oplus B_{3u}$
A_2	$A_u \oplus B_{3g}$
B_1	$B_{1g} \oplus B_{2u}$
B_2	$B_{1u} \oplus B_{2g}$

shows that each of the rovibronic states of $Si(H_2)Si$ can be split into two nondegenerate sublevels by tunneling between the two (A) and (B) forms.

The nuclear spin wave functions of $Si(H_2)Si$ generate the representation $3A_g \oplus B_{2u}$. The usual arguments show that the symmetry of the complete internal wave function of $^{28}Si(H_2)^{28}Si$ can only correspond to either the B_{2g} or B_{2u} species. Consequently, only the rotational states belonging to the $A_{g,u}$ and $B_{2g,2u}$ symmetry species are populated; the others are missing. The pure rotational spectrum (μ_c type) is that of a rigid asymmetric top with a dipole moment of A_u species. Using these results and the symmetry species of the rotational levels in $\mathscr{C}_{2v}(M)$, one can conclude that no splitting can be observed in this case. For the isotopically substituted $^{28}Si(D_2)^{28}Si$, the nuclear spin wave functions generate the representation $6A_g \oplus 3B_{2u}$ and the allowed irreducible representations of the complete internal wave function are either A_g or A_u. The same sublevels are populated for $^{28}Si(D_2)^{28}Si$ and no splitting can be observed. For the isotopomers $^{29}Si(H_2)^{28}Si$ and $^{30}Si(H_2)^{28}Si$, the CNPI group $\mathscr{C}_{2v}(M)$ is $\{E, (12), E^*, (12)^*\}$ and the MS group $[\mathscr{C}_s(M)]$ of one of the two (A) or (B) form is $\{E, (12)^*\}$, isomorphic to the $\mathscr{C}_s$ point group. The reverse correlation table from $\mathscr{C}_s(M)$ to $\mathscr{C}_{2v}(M)$:

$\mathscr{C}_s(M)$	$\mathscr{C}_{2v}(M)$
A	$A_1 \oplus B_1$
B	$A_2 \oplus B_2$

shows that the rovibronic states of $^{29}Si(H_2)^{28}Si$ or $^{30}Si(H_2)^{28}Si$ are split into two nondegenerate sublevels. The nuclear spin wave functions generate the representation $3A_1 \oplus B_2$ and, in that case, there are no missing levels. Then, a splitting is predicted with a 1:3 intensity ratio.

The predicted intensity ratio of the two components of a rotational line J', K_a', $K_c' \leftarrow J''$, K_a'', K_c'' in $^{28}Si(H_2)^{28}Si$, $^{29}Si(H_2)^{28}Si$, $^{30}Si(H_2)^{28}Si$, and $^{28}Si(D_2)^{28}Si$ are

K_a''	K_c''	$^{28}Si(H_2)^{28}Si$	$^{29}Si(H_2)^{28}Si$ $^{30}Si(H_2)^{28}Si$	$^{28}Si(D_2)^{28}Si$
Even or odd	Even	0/1	1/3	0/6
Even or odd	Odd	0/3	1/3	0/3

TABLE X. Experimental molecular constants of the different isotopomers of dibridged $Si(H_2)Si$.

	$^{28}Si(H_2)^{28}Si$	$^{29}Si(H_2)^{28}Si$	$^{30}Si(H_2)^{28}Si$	$^{28}Si(D_2)^{28}Si$
A (MHz)	157 198.866 8(76)	157 160.585 0(91)	157 124.909(23)	80 575.192 0(80)
B (MHz)	7281.326 47(75)	7157.938 5(30)	7042.832 7(34)	7180.278 25(75)
C (MHz)	7199.733 96(72)	7079.143 9(30)	6966.602 9(35)	7014.327 80(76)
Δ_J (kHz)	5.697 68(84)	5.516 2(38)	5.3468(48)	5.1716(11)
Δ_{JK} (kHz)	−61.704(17)	−61.829(43)	−61.79(13)	−1.897(21)
Δ_K (kHz)	8844.6(23)	8844.6[a]	8844.6[a]	2251.58(79)
δ_J (kHz)	−0.004 247(26)	−0.004 247[a]	−0.004 247[a]	0.004 29(15)
δ_K (kHz)	62.57(28)	62.57[a]	62.57[a]	52.40(11)
Φ_{JK}[b] (Hz)	0.607(81)	0.607[a]	0.607[a]	0.281(19)
Φ_{KJ}[b] (Hz)	−62.1(30)	−62.1[a]	−62.1[a]	−17.7(11)
Φ_K[b] (kHz)	1.04(17)	1.04[a]	1.04[a]	0.226(19)
σ (kHz)	21	54	61	19

[a]These parameters were fixed to the values obtained for $^{28}Si(H_2)^{28}Si$.
[b]Sextic centrifugal distortion constants other than Φ_{JK}, Φ_{KJ}, and Φ_K could not be determined and were fixed to zero.

However, no splitting has been experimentally observed for $^{29}Si(H_2)^{28}Si$, and $^{30}Si(H_2)^{28}Si$. Then, *ab initio* calculations have been performed to explain this. State-of-the-art *ab initio* calculations of barrier heights are known to be highly accurate.[64,65] The one-dimensional inversion coordinate of $Si(H_2)Si$ was chosen to be the distance between the Si···Si and H···H midpoints.[66] Consequently, the barrier height of this inversion motion calculated *ab initio* corresponds to the energy difference between the C_{2v} equilibrium structure of $Si(H_2)Si$ and the planar dibridged transition state of D_{2h} symmetry. Since the TZ2P CISD optimized geometry almost coincides with the r_s structure of $Si(H_2)Si$ determined in this study, all single-point barrier height calculations, reported in Table VI were chosen to be performed at this geometry and at the TZ2P CISD optimized D_{2h} structure (for the latter structure, r_{Si-Si}=2.3641 Å, and r_{Si-H}=1.5871 Å). Although the calculated barrier heights differ considerably at the different levels of theory (the largest value, 7457 cm^{-1}, was obtained at the 6-31G* SCF level, while the smallest one, 3502 cm^{-1}, at the TZ2P MP∞ level), enough data have been collected (see Table VI) to ascertain that the barrier height obtained at the cc-pVQZ CCSD(T) level, 3947 cm^{-1}, should be accurate to within 250 cm^{-1}. Naturally, this equilibrium value should be corrected for the effects of zero-point vibrations (ZPVE). Assuming a one-dimensional motion, a preliminary estimate of ZPVE is +563 cm^{-1}, based on the TZ2P+f CCSD(T) frequency data of Grev and Schaefer.[22] This means that the final estimate of the effective barrier height of the one-dimensional inversion motion of $Si(H_2)Si$ is 4500±300 cm^{-1}.

To obtain reasonable theoretical estimates of the inversion potential $[V(x)]$ and the inversion splittings, restricted geometry optimizations have been performed at the DZP MP2 level choosing the x inversion coordinate to be, as before, the distance between the Si···Si and H···H midpoints. The inexpensive DZP MP2 level was chosen for the theoretical calculations as the DZP MP2 bare barrier height, 4245 cm^{-1}, is slightly lower than the best estimate of the effective barrier height, 4500±300 cm^{-1}. During the restricted geometry optimizations the value of x was fixed ($x \in \{0, 1.2\}$, $\Delta x = 0.1$ Å). The discrete DZP MP2 energy points can be approximated to better than 2 cm^{-1} with the following model inversion potential: $V(x) = 4247 - 14\,452x^2 + 7977x^4 + 16\,430x^6 - 20\,945x^8 + 10\,604x^{10} - 2089x^{12}$, where x is measured in Å and V in cm^{-1}. The remarkably successful method of discrete variable representations (DVR) has been used to setup the vibrational Hamiltonian in one dimension,[67–71] employing (a) reduced dimensionless coordinates;[72] (b) a Gauss–Hermite basis function set; and

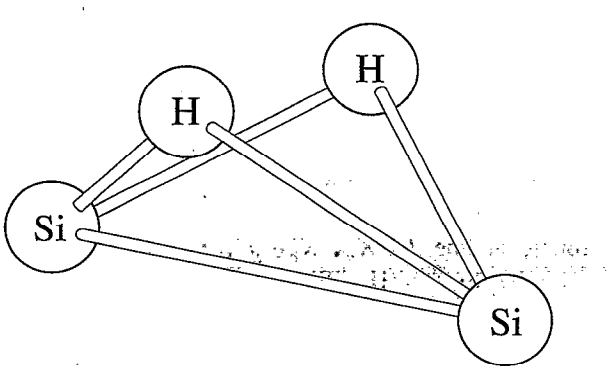

FIG. 5. Structure of $Si(H_2)Si$: Si–Si=2.2154 Å, Si–H=1.6680 Å, ∠HSiSiH =104.22°.

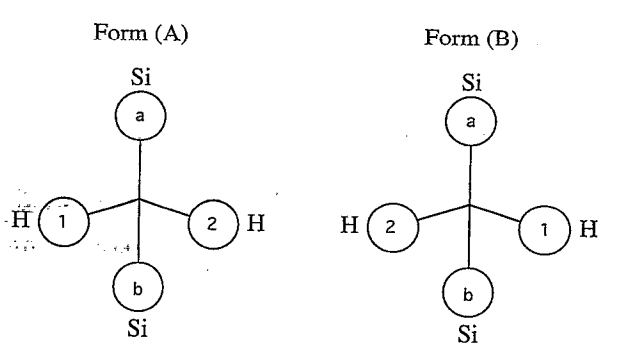

FIG. 6. The two symmetrically equivalent structures.

(c) an average reduced mass of 0.51 amu. Convergence for the first six eigenvalues is achieved by the time 59 optimized basis functions are used. The following splittings have been determined: $0^s-0^a=0.0239\ cm^{-1}$, $1^s-1^a=2.12\ cm^{-1}$, and $2^s-2^a=62.2\ cm^{-1}$. The predicted value for the ground state is large enough to induce observable splittings of the rotational lines. However, experimental observation of this inversion splitting appears to be difficult in view of the low S/N ratio obtained on the $^{29}Si(H_2)^{28}Si$ and $^{30}Si(H_2)^{28}Si$ lines observed in natural abundance and of the 1:3 intensity ratio of the two components.

V. CONCLUSION

The study of a silane plasma by high resolution millimeter-wave spectroscopy led to the experimental discovery of dibridged disilyne $Si(H_2)Si$. The observation of four different isotopomers $^{28}Si(H_2)^{28}Si$, $^{29}Si(H_2)^{28}Si$, $^{30}Si(H_2)^{28}Si$, and $^{28}Si(D_2)^{28}Si$ allowed the determination of a substitution structure. The geometry parameters obtained are in very good agreement with their *ab initio* counterparts. A group theory analysis of a possible inversion motion showed that splitting of the lines with a 1:3 intensity ratio should occur for the ^{29}Si and ^{30}Si isotopic monosubstitution. However, no splitting was experimentally detected with our standard sensitivity.

ACKNOWLEDGMENTS

The experimental part of the research, performed in Lille, France, was partially supported by the European Communities through Project No. 892 001 59/OP1 and by the C.N.R.S. (G.D.R. "Physico-Chimie des Molécules Interstellaires"). The authors wish to thank J. C. Guillemin (Laboratoire de Physico-Chimie Structurale, Université de Rennes 1) for synthesizing SiD_4, and B. Sombret (Laboratoire de Spectrochimie Infrarouge et Raman, Université des Sciences et Technologies de Lille) for recording the infrared spectrum of the deposits. The theoretical part of the research, performed in Budapest, Hungary, was partially supported by a grant from the Scientific Research Foundation of Hungary (OTKA 2101). Most of the *ab initio* calculations have been performed on an IBM RS/6000 m560 workstation whose purchase was made possible by a grant from "Catching Up with European Higher Education" (FEFA II/265). The authors wish to thank Professor G. Lucovsky for allowing us to reproduce Fig. 4(b) of G. Lucovsky, R. J. Nemanich, and J. C. Knights, Phys. Rev. B **19**, 2064 (1979), and Dr. V. Szalay for helpful discussions concerning calculation of inversion barriers.

[1] Y. P. Viala, Astron. Astrophys. Suppl. Ser. **64**, 391 (1986).
[2] E. Herbst and C. M. Leung, Astrophys. J. Suppl. **69**, 271 (1989).
[3] P. Thaddeus, S. E. Cummins, and R. A. Linke, Astrophys. J. **283**, L45 (1984).
[4] J. Cernicharo, C. A. Gottlieb, M. Guélin, P. Thaddeus, and J. M. Vrtilek, Astrophys. J. **341**, L25 (1989).
[5] M. Ohishi, N. Kaifu, K. Kawaguchi, A. Murakami, S. Saito, S. Yamamoto, S. I. Ishikawa, Y. Fujita, Y. Shiratori, and W. M. Irvine, Astrophys. J. **345**, L83 (1989).
[6] C. A. Gottlieb, J. M. Vrtilek, and P. Thaddeus, Astrophys. J. **343**, L29 (1989).
[7] J. Cernicharo, M. Guélin, C. Kahane, M. Bogey, C. Demuynck, and J. L. Destombes, Astron. Astrophys. **246**, 213 (1991).
[8] L. Muetterties, *Boron Hydride Chemistry* (Academic, New York, 1975).
[9] M. W. Crofton, M. F. Jagod, B. D. Rehfuss, and T. Oka, J. Chem. Phys. **91**, 5139 (1989).
[10] M. Bogey, M. Cordonnier, C. Demuynck, and J. L. Destombes, Astrophys. J. **399**, 103 (1992).
[11] E. P. Kanter, Z. Vager, G. Both, and D. Zajfman, J. Chem. Phys. **85**, 7487 (1986).
[12] M. Bogey, H. Bolvin, C. Demuynck, and J. L. Destombes, Phys. Rev. Lett. **66**, 413 (1991).
[13] B. Wirsam, Theor. Chim. Acta **25**, 169 (1972).
[14] P. H. Blustin, J. Organomet. Chem. **105**, 161 (1976).
[15] L. C. Snyder, Z. R. Wasserman, and J. W. Muskovitz, Int. J. Quantum Chem. **21**, 565 (1982).
[16] F. Kawai, T. Noro, A. Murakami, and K. Ohno, Chem. Phys. Lett. **92**, 479 (1982).
[17] H. Lischka and H. J. Köhler, J. Am. Chem. Soc. **105**, 6646 (1983).
[18] J. Kalcher, A. Sax, and G. Olbrich, Int. J. Quantum Chem. **25**, 543 (1984).
[19] (a) J. S. Binkley, J. Am. Chem. Soc. **106**, 603 (1986); (b) P. Ho, M. E. Coltrin, J. S. Binkley, and C. F. Melius, J. Phys. Chem. **90**, 3399 (1986).
[20] D. A. Clabo and H. F. Schaefer III, J. Chem. Phys. **84**, 1664 (1986).
[21] B. T. Colegrove and H. F. Schaefer III, J. Phys. Chem. **94**, 5593 (1990).
[22] R. S. Grev and H. F. Schaefer III, J. Chem. Phys. **97**, 7990 (1992).
[23] L. A. Curtiss, K. Raghavachari, P. W. Deutsch, and J. A. Pople, J. Chem. Phys. **95**, 2433 (1991).
[24] M. M. Hühn, R. D. Amos, R. Kobayashi, and N. C. Handy, J. Chem. Phys. **98**, 7107 (1993).
[25] M. Cordonnier, M. Bogey, C. Demuynck, and J. L. Destombes, J. Chem. Phys. **97**, 7984 (1992).
[26] W. H. Press, B. P. Flannery, S. A. Teukolsky, and W. T. Vetterliing, *Numerical Recipes. The Art of Scientific Computing* (Cambridge University Press, New York, 1986).
[27] G. Lucovsky, R. J. Nemanich, and J. C. Knights, Phys. Rev. B **19**, 2064 (1979).
[28] R. Robertson and A. Gallagher, J. Appl. Phys. **59**, 3402 (1986).
[29] (a) W. J. Hehre, R. Ditchfield, and J. A. Pople, J. Chem. Phys. **56**, 2257 (1972); (b) P. C. Hariharan and J. A. Pople, Theor. Chim. Acta **28**, 213 (1973); (c) Mol. Phys. **27**, 209 (1974).
[30] (a) S. Huzinaga, J. Chem. Phys. **42**, 1293 (1965); (b) *Approximate Atomic Functions* (Department of Chemistry Report, University of Alberta, Edmonton, 1971), Vol. 2.
[31] T. H. Dunning, J. Chem. Phys. **53**, 2823 (1970).
[32] T. H. Dunning, J. Chem. Phys. **55** 716 (1971).
[33] A. D. McLean and S. Chandler, J. Chem. Phys. **72**, 5639 (1980).
[34] (a) T. H. Dunning, J. Chem. Phys. **90**, 1007 (1989); (b) R. A. Kendall, T. H. Dunning, and R. J. Terrison, *ibid.* **96**, 6796 (1992).
[35] D. Woon and T. H. Dunning (unpublished results).
[36] T. J. Lee and P. R. Taylor, Int. J. Quantum Chem., Quantum Chem. Symp. **23**, 199 (1989).
[37] C. C. J. Roothaan, Rev. Mod. Phys. **23**, 69 (1951).
[38] A. Szabó and N. S. Ostlund *Modern Quantum Chemistry* (McGraw–Hill, New York, 1989).
[39] C. Møller and M. S. Plesset, Phys. Rev. **46**, 618 (1934).
[40] (a) R. Krishnan, M. J. Frisch, and J. A. Pople, J. Chem. Phys. **72**, 4244 (1980); (b) W. J. Hehre, L. Radom, P. V. R. Schleyer, and J. A. Pople, *Ab Initio Molecular Orbital Theory* (Wiley–Interscience, New York, 1986).
[41] (a) R. J. Bartlett, Annu. Rev. Phys. Chem. **32**, 359 (1981); (b) R. J. Bartlett, C. E. Dykstra, and J. Paldus, in *Advanced Theories and Computational Approaches to the Electronic Structure of Molecules*, edited by C. E. Dykstra (Reidel, Dordrecht, 1984), p. 127.
[42] I. Shavitt, in *Methods in Electronic Structure Theory*, edited by H. F. Schaefer III (Plenum, New York, 1977), p. 189.
[43] (a) P. Saxe, D. J. Fox, H. F. Schaefer III, and N. C. Handy, J. Chem. Phys. **77**, 5584 (1982); (b) J. P. Goddard, N. C. Handy, and H. F. Schaefer III, *ibid.* **71**, 1525 (1979); (c) Y. Osamura, Y. Yamaguchi, and H. F. Schaefer III, *ibid.* **75**, 2919 (1981).
[44] S. Kucharski and R. J. Bartlett, Adv. Quantum Chem. **18**, 281 (1986).
[45] (a) G. E. Scuseria, A. C. Scheiner, T. J. Lee, J. E. Rice, and H. F. Schaefer III, J. Chem. Phys. **86**, 2881 (1987); (b) A. C. Scheiner, G. E. Scuseria, J. E. Rice, T. J. Lee, and H. F. Schaefer III, *ibid.* **87**, 5361 (1987).
[46] K. Raghavachari, G. W. Trucks, J. A. Pople, and M. Head-Gordon, Chem. Phys. Lett. **157**, 479 (1989).
[47] G. E. Scuseria and T. J. Lee, J. Chem. Phys. **93**, 5851 (1990).

[48] S. R. Langhoff and E. R. Davidson, Int. J. Quantum Chem. **8**, 61 (1974).
[49] J. A. Pople, M. J. Frisch, B. T. Luke, and J. S. Binkley, Int. J. Quantum Chem., Quantum Chem. Symp. **17**, 307 (1983).
[50] N. C. Handy, P. J. Knowles, and K. Somasundram, Theoret. Chim. Acta **68**, 87 (1985).
[51] PSI 2.0, 1991, PSITECH, Inc., Watkinsville, GA.
[52] J. F. Stanton, J. Gauss, J. D. Watts, W. J. Lauderdale, and R. J. Bartlett, Int. J. Quantum Chem., Quantum Chem. Symp. **26**, 879 (1992).
[53] J. K. G. Watson, J. Mol. Spectrosc. **41**, 229 (1972).
[54] X. F. Zhou and P. Pulay, J. Comput. Chem. **10**, 935 (1989).
[55] A. G. Császár, J. Phys. Chem. **96**, 7898 (1992).
[56] W. D. Allen and A. G. Császár, J. Chem. Phys. **98**, 2983 (1993).
[57] W. D. Allen, Program INTDER, Version 1.0, Stanford University, Stanford, CA.
[58] D. Papousek and M. R. Aliev, *Molecular Vibrational–Rotational Spectra* (Elsevier, Amsterdam, 1982).
[59] M. R. Aliev and J. K. G. Watson, in *Molecular Vibrational–Rotational Spectra*, edited by K. N. Rao (Academic, New York, 1985), Vol. 3, p. 1.
[60] W. D. Allen, Y. Yamaguchi, A. G. Császár, A. D. Clabo, Jr., R. B. Remington and H. F. Schaefer III, Chem. Phys. **145**, 427 (1990).
[61] A. D. Clabo, Jr., W. D. Allen, R. B. Remington, Y. Yamaguchi, and H. F. Schaefer III, Chem. Phys. **123**, 427 (1988).
[62] J. K. G. Watson, in *Vibrational Spectra and Structure*, edited by J. R. Durig (Elsevier, Amsterdam, 1977), Vol. 6, p. 2.
[63] A. G. Császár and G. Fogarasi, J. Chem. Phys. **89**, 7646 (1988).
[64] W. D. Allen, A. G. Császár, and D. A. Horner, J. Am. Chem. Soc. **114**, 6834 (1992).
[65] W. D. Allen, A. L. L. East, and A. G. Császár, in *Structures and Conformations of Non-Rigid Molecules*, edited by J. Laane, M. Dakkouri, B. Van der Veken, and H. Oberhammer (Kluwer, Dordrecht, 1993), p. 343.
[66] D. Gremer and J. A. Pople, J. Am. Chem. Soc. **97**, 1354 (1975).
[67] J. C. Light, I. P. Hamilton, and J. V. Lill, J. Chem. Phys. **82**, 1400 (1985).
[68] Z. Bacic and J. C. Light, Annu. Rev. Phys. Chem. **40**, 469 (1989).
[69] V. Szalay, J. Chem. Phys. **99**, 1978 (1993).
[70] D. O. Harris, G. G. Engerholm, and W. D. Gwinn, J. Chem. Phys. **43**, 1515 (1965).
[71] A. S. Dickinson and P. R. Certain, J. Chem. Phys. **49**, 4209 (1968).
[72] (a) T. B. Malloy, J. Mol. Spectrosc. **44**, 504 (1972); (b) T. B. Malloy and W. J. Lafferty, *ibid.* **54**, 20 (1975).